An improved method for measuring soil N2O fluxes using a quantum cascade laser with a dynamic chamber

Cowan, NJ; Famulari, D; Levy, PE; Anderson, M; Bell, MJ; Rees, RM; Reay, DS; Skiba, UM

Published in:
European Journal of Soil Science

DOI:
10.1111/ejss.12168

Print publication: 01/01/2014

Document Version
Peer reviewed version

An improved method for measuring soil N_2O fluxes using a quantum cascade laser with a dynamic chamber

N. J. Cowan [a, b*], D. Famulari [a], P. E. Levy [a], M. Anderson [a], M. J. Bell [c], R. M. Rees [c], D. S. Reay [b] & U. M. Skiba [a]

[a]Centre for Ecology and Hydrology, Edinburgh, [b]School of Geosciences, University of Edinburgh, Edinburgh, and [c] Scotland's Rural University College, Edinburgh

**Correspondence: N. Cowan. Email: nicwan11@ceh.ac.uk*

Running title: Dynamic chamber method.

Keywords: nitrous oxide, chamber, methodology, regression

Summary

A dynamic chamber method was developed to measure fluxes of N_2O from soils with greater accuracy than previously possible, through the use of a quantum cascade laser (QCL). The dynamic method was compared with the conventional static chamber method, where samples are analysed subsequently on a gas chromatograph. Results suggest that the dynamic method is capable of measuring soil N_2O fluxes with an uncertainty of typically less than 1–2 µg N_2O-N m^{-2} $hour^{-1}$ (0.24–0.48 g N_2O-N ha^{-1} day^{-1}), much less than the conventional static chamber method, because of the greater precision and temporal resolution of the QCL. The continuous record of N_2O and CO_2 concentration at 1 Hz during chamber closure provides an insight into the effects that enclosure time and the use of different regression methods may introduce when employed with static chamber systems similar in design. Results suggest that long enclosure times can contribute significantly to uncertainty in chamber flux measurements. Nonlinear models are less influenced by effects of long enclosure time, but even these do not always adequately describe the observed concentrations when enclosure time exceeds 10 minutes, especially with large fluxes.

Introduction

Nitrous oxide (N_2O) is a potent greenhouse gas (GHG) and the single largest contributor to global stratospheric ozone depletion (Ravishankara *et al.*, 2009). The majority of N_2O is released into the atmosphere by the natural microbial processes of nitrification and denitrification (e.g. Davidson *et al.*, 2000), but human activities (such as the wide scale use of nitrogen fertilizers) have resulted in a significant increase in global N_2O emissions since pre-industrial times (IPCC, 2007). Global N_2O fluxes have large uncertainties associated with them (55–75 %) (IPCC, 2007) because of the large temporal and spatial variability of N_2O fluxes, and the uncertainty inherent in the methodology predominantly used to measure them (Folorunso & Rolston, 1985; Velthof *et al.*, 1996).

Almost all measurements use the closed, non-steady-state (or 'static') chamber method (Hutchinson & Mosier, 1981), because of its simplicity and small cost (de Klein & Harvey, 2013). In this method, gas samples are extracted from a chamber sealed on the soil surface during a 30–60 minute incubation period, and later analysed using a gas chromatograph (GC) instrument. The flux is inferred from the rate of change in gas concentration within the chamber. Because of the constraints imposed by the logistics of extracting samples and subsequent laboratory analysis, the sample size is typically limited to 2–4 samples per chamber closure. Consequently the fluxes calculated by any regression model are poorly constrained (Pedersen *et al.*, 2010). Furthermore, data can be noisy, and it is not always clear which regression model is the most appropriate for fitting to the data (Levy *et al.*, 2011). The resolution of GC instruments tends to be poor (>10 nmol mol^{-1} for N_2O), meaning that small fluxes may not be clearly detectable.

Previous attempts to improve the precision of N_2O flux measurements, using infrared spectroscopy to measure concentration changes of N_2O within chambers, were limited by the

poor resolution of the instruments available (Yamulki & Jarvis, 1999; Laville *et al.*, 2011), the logistical constraints of operation, and cost (Hensen *et al.*, 2006; Hensen *et al.*, 2013). However, advances in infrared laser technology have recently produced fast-response (> 10 Hz) N_2O analysers with improved sensitivity (< 5 nmol mol^{-1}), capable of operating in the field (Laville *et al.*, 1999; Jones *et al.*, 2011). In this study, we used a commercially-available infrared continuous wave quantum cascade laser (QCL) with a resolution of 30 pmol mol^{-1}. Pulsed QCL instruments (resolution of 1.5 nmol mol^{-1}) have been used successfully to measure N_2O fluxes using the eddy covariance method (Eugster *et al.*, 2007; Kroon *et al.*, 2007; Kort *et al.*, 2011). The objective of this work was to incorporate this instrument into a dynamic non-steady-state chamber design, which allows for significantly improved accuracy and precision when measuring N_2O fluxes. This method would also then be able to verify measurements made with less precise methodologies such as static chambers. In this paper we describe the system design, the analysis of the high-resolution data obtained, and comparison with conventional static chamber measurements. Costs and benefits of the dynamic chamber/QCL system are compared with the conventional static chamber system.

Materials and methods

We constructed a non-steady-state flow-through (or dynamic) chamber system (Livingston & Hutchinson, 1995; Hensen *et al.*, 2006) hereafter referred to as the dynamic chamber method, in which a closed volume of air was circulated between a chamber and the QCL gas analyser *via* a pump (Figure 1). A compact continuous wave quantum cascade laser (CW-QC-TILDAS-76-CS, Aerodyne Research Inc., Billerica, MA, USA) was used to measure gas

concentrations within the chamber. This instrument uses tuneable infrared differential absorption spectroscopy (Zahniser *et al.*, 2009), with a 0.5-litre multi-pass absorption cell, with an optical path length of 76 metres. The laser source requires a very stable temperature to operate, and a solid-state cooling system (Thermocube, SS cooling systems, New York, USA) kept the system at a constant temperature of 10˚ C by pumping a cooled solution of water and ethanol (20%). The cell was kept at a constant low pressure (approximately 45 Torr) using a dry-scroll vacuum pump (SH-110, Varian Vacuum Technologies, Lexington MA, USA). The inlet of the QCL was fitted with a manual ball valve and a needle valve to control the air flow rate and cell pressure, as well as a safety valve attached to the pump to prevent back-flow. A 0.45-micron particle filter was attached to the inlet of the absorption cell.

The chamber consisted of a cylindrical polyvinyl chloride (PVC) plastic pipe of 38-cm inner diameter (ID) and 22- cm height. The chamber had PVC flanges fitted at the top and bottom. A 3-mm thick square aluminium metal lid was fitted to the top of the tube and sealed with epoxy resin and silica sealant. A 1-cm layer of closed cell neoprene sponge was fitted around the bottom flange. The chamber was placed onto a collar which could be inserted several cm into the soil (on average 5 cm). The collar consisted of a PVC flange attached to a stainless steel ring (2-mm thickness, 6-cm height). The closed cell neoprene sponge attached to the underside of the chamber formed an airtight seal with the collar.

The chamber was fitted with an internal fan (3000 rpm, Delta Electronics Inc., Taipei, Taiwan) and air temperature probe (CS109, Campbell Scientific, Logan, UT, USA). A pressure sensor (CS100, Campbell Scientific, UT, USA) fitted to the lid of the chamber measured the internal air pressure. All fittings on the lid of the chamber were sealed with silicone sealant to avoid gas leakage. The temperature and pressure sensors were connected to a data logger (CR1000, Campbell Scientific, UT, USA) which stored data every second. The

chamber was fitted with a rubber flap (1-mm thickness, 6-cm width) which could be rolled down to shield the seal formed between the neoprene sponge and the base of the collar or chamber from wind.

Two 30-m lengths of 9.5 mm ID Tygon® tubing were attached to both the inlet of the QCL and the outlet of the pump. This provided a 30-m radius from the QCL in which the chamber could be placed. Tygon® tubing was used as it allowed flexibility in the movement of the chamber and does not interact with N_2O. A flow rate of approximately 6 to 7 l minute^{-1} was used between the QCL and the chamber. There was a lag time of approximately 20 seconds between gas leaving the chamber and entering the analyser. Prior to each measurement, the chamber was purged with ambient air for one minute, and the data for the first minute following closure was discarded. The chamber volume was estimated after each measurement by recording depth from the chamber top to the soil surface at ten points. The typical volume of the enclosed system was 0.03 m^3 with a cross sectional area of 0.12 m^2.

To investigate the effect that circulating air through the chamber had on internal pressure, we made measurements in the lab with the chamber sealed on an impermeable metal base. Care was taken to ensure that the chamber was completely sealed by using strong clamps and bolts to seal between the neoprene layer and the metal base. In these measurements, the chamber was fitted with a very sensitive differential pressure sensor (PX654, Omega Engineering Inc., Stamford, CT, US) with a precision of 0.1 Pa. A flow rate of 6 l minute^{-1} reduced pressure in the chamber by approximately 3 Pa (because of the drop in static pressure with fluid speed). This drop in pressure was considered to be negligible when compared to the natural variation in air pressure caused by wind and temperature variation (> 100 Pa).

Field measurements were made at two locations. Firstly, we measured on grass turf at our institute (near Penicuik, Scotland, 55° 51' 42.827"N, 3° 12' 21.6393"W), where we

enhanced N_2O fluxes by applying 50 g of ammonium nitrate dissolved in 5 litres of water and spread over 10 m^2 (17.5 kg N ha^{-1}). Four collar rings were inserted into the treated area and one collar ring was inserted into an untreated area as a control. Measurements were made from each of the five chambers on four separate days, each lasting approximately one hour. Secondly, we made measurements in a grazed field using both chamber methods from the same collars at Crichton near Dumfries, SW Scotland (55° 2' 31.3238"N, 3° 35' 16.4393"W) where different fertilizer types (synthetic urine, cattle urine, cattle urine mixed with dicyandiamide (DCD) and cattle dung) had been applied at rates of 425, 435, 435 and 720 kg N ha^{-1} respectively.

Fluxes of N_2O were calculated using linear and non-linear asymptotic regression methods (Equations (1)–(4)) using the HMR package for the statistical software R (Pedersen *et al.*, 2010). The regression method that provided the best fit for the time series of concentration was chosen for each individual measurement, using goodness-of-fit statistics and visual inspection.

(i) Linear regression. Fluxes are calculated using the standard line of best fit through the data:

$$C_t = a + b \times t, \quad (1)$$

where C_t is the gas concentration at time t, and dC/dt is:

$$\frac{dC}{dt_0} = b \ . \quad (2)$$

(ii) HM model. This is a commonly used non-linear model derived by Hutchinson & Mosier (1981) with a negative exponential form of curvature. The change in C with t is given by:

$$C_t = C_{max} - (C_{max} - C_0)\exp(-kt), \quad (3)$$

where C_0 is the initial concentration, C_{max} is the value at equilibrium and k is a constant, and calculates dC/dt_0 as:

$$\frac{dC}{dt_0} = k(C_{max} - C_0) \ . \quad (4)$$

Once the rate of change in concentration of a particular gas is known it can then be used to calculate soil flux for each measurement (See Equation (5)). The flux can then be converted to the appropriate units by simple unit conversion factors.

$$F = \frac{dC}{dt_0} \cdot \frac{\rho V}{A}, \quad (5)$$

where F is gas flux from the soil (nmol m^{-2} s^{-1}), dC/dt_0 is the initial rate of change in concentration with time in nmol mol^{-1} $s^{-1,}$ ρ is the density of air in mol m^{-3}, V is the volume of the chamber in m^3 and A is the ground area enclosed by the chamber in m^2.

Static chamber measurements were made at the Crichton site using identical chambers, following an existing protocol (see www.GHGPlatform.org.uk). Chambers were sealed for 40 minutes, then a single sample taken *via* a three-way tap in the lid. All gas samples were collected with a 20-ml syringe and stored in evacuated 20-ml glass vials. Rather than sampling gas concentration at the time of closure, this was estimated from 10 samples of ambient air collected during the measurement day. All of the samples were analysed on a 7890A GC System fitted with an ECD and FID detector (Agilent Technologies, Santa Clara, CA, USA) at SRUC. The concentration change inside the static chambers was calculated by subtracting the concentration of N_2O measured within the chamber (at t = 40 minutes) from the daily average ambient N_2O concentration. Using Equation (5), the flux of N_2O from each chamber was calculated assuming that the concentration change within the chamber was linear. The static and dynamic chamber methods were compared by measuring on the same collars on the same day or within 24 hours. Static chamber measurements were carried out in the early morning, and then dynamic chamber measurements were made throughout the day.

Results and discussion

Effects of wind

In initial tests, strong gusts of wind (> 10 m s^{-1}) did have a clear influence on the observed concentrations within the chamber, presumably by inducing air flow between the neoprene gasket and the collar (Figure 2). To counter this, a ring of rubber made from a bicycle inner-tube was used to form a skirt which could be rolled to cover the seal between the chamber and the collar. Subsequent to fitting this skirt, no further effects of wind on the concentrations within the chamber were observed, and the concentration pattern was as shown in Figure 3. Effects of wind were only observable with the high frequency concentration measurements from the QCL, and would not be detected in conventional static chambers, where concentration measurements are made at much lower time frequency (> 600 seconds).

The influence of enclosure time on calculated flux

Figure 4 shows the concentration increase within the chamber over the course of twenty one hour-long measurements made on metal collars inserted into fertilized grassland soil. The plots are ranked in order of magnitude of flux calculated using linear regression, increasing top-left to bottom-right (labelled 1 to 20 in sequential measurement order). The plots show that there is little noise in the measurements, and the clear pattern in concentration with time, irrespective of the magnitude of the flux. Almost all of the concentration changes appear to be close to linear with time, with only a few exceptions. The fluxes calculated from the chambers over a 60-minute measurement period using linear and non-linear regression are shown in Table 1. The R^2 values for both linear and non-linear fits exceed 0.99 for most of the

206 measurements; however, there are significant differences in the flux calculated using the
207 different regression methods. Flux calculated using linear regression is smaller than those
208 calculated using non-linear regression for all 20 measurements. The 95% confidence intervals
209 estimated from the fitted regressions are also shown in Table 1.

210 Figure 5 shows the fluxes calculated from these data over a range of possible
211 enclosure times, and with both linear and non-linear fitted models. Despite the appearance of
212 linearity in Figure 4, the calculated fluxes for the different time periods deviate from the flux
213 calculated after three minutes, and this deviation generally increases with the magnitude of
214 the flux (note that the fluxes are all shown on the same absolute scale.) At the extreme, this
215 can be approximately 1.5 nmol m^{-2} s^{-1} or 40% of the flux. Although a non-linear model
216 should be much less sensitive to enclosure time, even this progressively deviates from the flux
217 calculated after three minutes. In two cases, the non-linear model deviates more than the
218 linear one (measurements 12 & 16), but in these instances, the curves are slightly convex, and
219 non-linear fitting to these data would usually be rejected.

220 We would conclude from these results that fluxes should be calculated using chamber
221 enclosure times of considerably less than one hour. Whilst an effect of enclosure time might
222 be expected if using a linear model whenever there is any degree of curvature in the rate of
223 change in concentration, this is not expected when using a non-linear model. In principle, a
224 non-linear model should account for the effects of feedbacks which change the rate of change
225 in concentration over time (most obviously, the build-up of N_2O within the chamber slows the
226 rate of diffusion from the soil, and increases the loss of N_2O to ambient air through any leaks
227 present). Our empirical results show that the variation in the rate of change in concentration
228 over time is not always well represented by any model. For example, while the curvature in
229 measurements 9, 13 & 18 is accounted for well, there are changes in curvature in
230 measurements 11 & 15 which are not captured by the model. Presumably this arises because

of some artefact of the chamber, measuring environment or instrument which changes over time.

On the basis of these results, we would suggest that the safest approach is to use a short enclosure time, typically less than five minutes, where model assumptions are best met. This seems to provide a sufficiently long-enough data-run to establish a good fit, and be short enough to reduce any measurement artefacts which may change over time. One might attempt to find an optimal enclosure time by assessing the marginal increase in information with change in goodness-of-fit as enclosure time increases. More simply, the model residuals can be plotted against enclosure time, and the longest enclosure time choosen where no trend is present in the residuals.

The choice of regression model used to calculate fluxes from chamber measurements is recognised as one of the largest sources of uncertainty (Kroon *et al.*, 2008; Pedersen *et al.*, 2010; Parkin *et al.*, 2012). We would also conclude that a non-linear model fit needs to be included whenever enclosure times are long, as they are more robust than the linear model to any artefact of enclosure time. It should be noted that statistical null-hypothesis testing of linear versus non-linear model fits is not pertinent, and failure to detect a statistical difference can be misconstrued as equivalence. For example, in measurement number 11, fluxes calculated by linear and non-linear models differ by 20%, but no statistically significant difference can be detected. With only three to five points as conventionally available from GC-based methods, there would be no chance of detecting any such statistical difference.

Comparison of dynamic and static chamber methods

Comparison of static and dynamic chambers at identical locations showed under-estimation in the flux measured with the static chamber measurements than from the dynamic chamber (R^2

value of 0.71); however this relationship is dominated by a small number of measurements with much influence (Figure 6). A bias towards smaller flux measurements using the static chamber method may arise because of the implicit assumption of linearity over the 40-minute enclosure time (there was only one sample taken, and an estimate of initial concentration). The lack of agreement between individual measurements using both methods in this experiment is probably caused by the large uncertainty in the static chamber method. Although there was inevitably some delay between measurements at the same locations by the two methods (typically one to five hours, but as much as 24 hours in a few cases), the time delay did not explain any of the difference in the measured fluxes. Nor was any pattern related to diurnal temperature change apparent in the differences.

Background fluxes measured in the non-fertilized control plots of the field experiment using the static chamber method ranged between -32 to 44 μg N_2O-N m^{-2} $hour^{-1}$. In comparison, fluxes measured from the same locations using the dynamic QCL method were consistently below 10 μg N_2O-N m^{-2} $hour^{-1}$, with calculated uncertainty of approximately 1 μg N_2O-N m^{-2} $hour^{-1}$. The mean flux values calculated from all control plot measurements from the dynamic and static chamber methods are 2.5 and 5.4 μg N_2O-N m^{-2} $hour^{-1}$, respectively, using linear regression. Both methods report similar mean flux values for the control plots; however the range of flux measurements from the control plots varies significantly between the methods (Figure 7). The small range of fluxes measured with the dynamic chamber suggests that the method is able to provide measurements of small N_2O flux with greater consistency and precision than the static chamber is able to.

Uncertainty calculation

For each measurement, we estimated the uncertainty associated with each of the terms in Equation (5), and propagated these to estimate the total uncertainty in the flux. Uncertainty in d*C*/d*t* was obtained from the 95% confidence interval in the regression slope parameter. Uncertainty in the chamber volume could be estimated by taking several measurements of height in each chamber, and taking the 95% confidence interval in the calculated chamber volume. Including estimates of the volume of vegetation, this gave values of approximately 10% of the total volume. Uncertainty in the air density term (ρ) arises from uncertainties in the temperature and pressure measurements. The 95% confidence interval for the mean temperature and pressure was calculated from the 1 Hz data, and added to the instrumental precision of the temperature probe (0.4°C) and pressure sensor (50 Pa). For the static chambers measurements, it was not possible to calculate regression uncertainty as concentration during chamber closure was only measured once. However, a previous study has estimated that the realistic confidence intervals based on uncertainty arising from instrumental errors and poor fitting to the model are typically of an order of 20% that of the measured flux, although this can vary substantially (Levy *et al.*, 2011).

The results of the one-hour long and the comparison measurements suggest that the uncertainty in flux due to d*C*/d*t* can be large (minimum of approximately 20 μg N_2O-N m^{-2} $hour^{-1}$) using the static chamber method, but is reduced to typically < 10 μg N_2O-N m^{-2} $hour^{-1}$ in the dynamic QCL chamber method. Uncertainties from the temperature and pressure measurements are small and should apply to both methods (ranging from 0 to 2.83 μg N_2O-N m^{-2} $hour^{-1}$). In the dynamic chamber method, only the volume term remains as a significant source of error; this is because errors in volume scale linearly with flux. Only occasionally does the uncertainty in d*C*/d*t* contribute significantly, where there is not a good relationship with concentration measurements (Figure 8).

304 The dynamic chamber used with the QCL provides more data than the static chamber
305 method from which uncertainties from individual chamber measurements can be confidently
306 estimated. This allows a detailed investigation of how to improve flux measurements as well
307 as providing a clearer picture of the true spatial variability of N_2O fluxes from soils. The
308 largest source of error in static chambers comes from estimating d*C*/d*t* (Levy *et al.*, 2011).
309 This uncertainty is not as large using the dynamic chamber method. The largest source of
310 error which could be eliminated from the dynamic chamber method is that of volume. The
311 volume uncertainty can be difficult to address on non-uniform soils. Paying more attention to
312 measuring the volume of vegetation and measuring the soil microtopography would be ways
313 to improve the chamber volume estimation, as simple steps to increase the accuracy of
314 chamber methods.
315
316 *Advantages and disadvantages*
317 The dynamic chamber method is adaptable and able to work with a variety of instruments and
318 chamber designs. A significant advantage of this particular arrangement is that the high-
319 precision laser instrument can be used for both micrometeorological measurements and
320 chambers alternately. The biggest advantage of linking this laser to a dynamic chamber over
321 conventional static chambers is the large resolution of N_2O concentration measurements.
322 Uncertainty calculated in the smallest flux measurements was typically less than 2 μg N_2O-N
323 m^{-2} $hour^{-1}$, defined as the 95% confidence interval in the estimate of the flux, and this may be
324 interpreted as a limit of detection for the measurement system (*sensu* Parkin *et al.*, 2012),
325 although definitions in the literature vary. The development of these methods is important to
326 improving the accuracy of GHG measurements which can then provide reliable information
327 on the efficacy of mitigation of N_2O from a variety of agricultural sources.

Currently the biggest drawbacks of using the QCL system are the initial setup cost and the power requirements of the system. The mobility of the instrumentation is limited as a mains power supply or generator is required, thus limiting the spatial coverage of the system. To avoid long lag times we limited the tubing to 30 metres, which limited the distance accessible for measurements. However, the QCL instrument is relatively robust to vibrations and temperature changes and is capable of being mounted in an off-road vehicle without significantly altering the detection limit of the system. A mobile system such as this would allow a wide area to be sampled. There are difficulties in using the dynamic chamber methods to make a large number of simultaneous measurements often demanded by field experiments comparing different treatments. However, because each measurement is short and no further laboratory analysis is required, we estimate that a larger number of flux measurements can be made per hour of effort (Table 2). Combined with the greater precision of the measurements, this yields an estimate of the mean or total flux from the sampled domain with less uncertainty than when using conventional static chambers.

The main disadvantages of the method are the large capital cost and the technical complexity of the instrument. With current trends in laser-based gas analysers, prices will decrease and ease-of-use will improve, and this gap between the methods will reduce.

Conclusions

Using precise, fast-response gas analysers such as a QCL in combination with chambers provides more reliable data than the conventional static chamber/GC approach. Fluxes and their associated physical and statistical uncertainties can be properly quantified, even when fluxes are very small (below 10 μg N_2O-N m^{-2} $hour^{-1}$). It is important that errors and

uncertainties in these systems are understood, and the dynamic chamber methodology gives us insights that were previously unavailable. The enhanced precision, ability to measure several gases including isotopologues will advance our understanding of soil processes and associated emissions of N_2O and CH_4. Dynamic and static chamber methods can deliver roughly the same number of flux measurements in the field (up to ten) within one hour, assuming four samples are withdrawn from static chambers within this one hour, but the dynamic chamber method has no subsequent laboratory sample analysis stage, which can take several days. Currently high costs, power consumption, weight and lack of portability limit the use of fast dynamic chamber approaches to measure N_2O or CH_4 fluxes. In time, these restrictions will be lessened, as developments in lower power laser technology become available.

Acknowledgements

We thank A. Bagnall (SRUC) for providing us with the chamber and flux data from the Crichton field site. We also thank DEFRA and the UK Devolved Administrations for financial support through the UK GHG Platform project AC0116 (The InveN_2Ory project).

References

Davidson, E.A., Keller, M., Erickson, H.E., Verchot, L.V., & Veldkamp, E. 2000. Testing a conceptual model of soil emissions of nitrous and nitric oxides. *Bioscience,* **50,** 667-680.

Eugster, W., Zeyer, K., Zeeman, M., Michna, P., Zingg, A., Buchmann, N. & Emmenegger, L. 2007. Methodical study of nitrous oxide eddy covariance measurements using quantum cascade laser spectrometery over a Swiss forest. *Biogeosciences*, **4,** 927-939.

Folorunso, O.A. & Rolston, D.E. 1985. Spatial and spectral relationships between field-measured denitrification gas fluxes and soil properties1. *Soil Science Society of America Journal*, **49,** 1087-1093.

Hensen, A., Groot, T.T., van den Bulk, W.C.M., Vermeulen, A.T., Olesen, J.E. & Schelde, K. 2006. Dairy farm CH_4 and N_2O emissions, from one square metre to the full farm scale. *Agriculture, Ecosystems & Environment*, **112,** 146-152.

Hensen, A., Skiba, U. & Famulari, D. 2013. Low cost and state of the art methods to measure nitrous oxide emissions. *Environmental Research Letters*, **8,** 025022.

Hutchinson, G.L. & Mosier, A.R. 1981. Improved soil cover method for field measurement of nitrous-oxide fluxes. *Soil Science Society of America Journal*, **45,** 311-316.

IPCC, 2007: *Climate Change 2007: The Physical Science Basis. Contribution of Working Group I to the Fourth Assessment Report of the Intergovernmental Panel on Climate Change.* (eds Solomon, S., Qin, D., Manning, M., Chen, Z., Marquis, M., Averyt, K.B., Tignor, M., *et al*). Cambridge University Press, Cambridge, United Kingdom.

Jones, S.K., Famulari, D., Di Marco, C.F., Nemitz, E., Skiba, U.M., Rees, R.M., *et al*. 2011. Nitrous oxide emissions from managed grassland: a comparison of eddy covariance and static chamber measurements. *Atmospheric Measurement Techniques*, **4,** 2179-2194.

de Klein, C. & Harvey, M., *et al*. 2013. Nitrous oxide chamber guidelines; Global Research Alliance on Agricultural Greenhouse Gases. (At: www.globalresearchalliance.org/research/livestock/activities/nitrous-oxide-chamber-methodology-guidelines/. Accessed: 16/6/14*)*

Kort, E.A., Patra, P.K., Ishijima, K., Daube, B.C., Jiménez, R., Elkins, J., *et al.* 2011. Tropospheric distribution and variability of N_2O: Evidence for strong tropical emissions. *Geophysical Research. Letters*, **38,** L15806.

Kroon, P.S., Hensen A., Jonker, H.J.J., Zahniser, M.S., van 't Veen, W.H. & Vermeulen, A.T. 2007. Suitability of quantum cascade laser spectroscopy for CH_4 and N_2O eddy covariance flux measurements. *Biogeosciences*, **4,** 715-728.

Kroon, P.S., Hensen, A., Bulk, W.C.M., Jongejan, P.A.C. & Vermeulen, A.T. 2008. The importance of reducing the systematic error due to non-linearity in N_2O flux measurements by static chambers. *Nutrient Cycling in Agroecosystems*, **82,** 175-186.

Laville, P., Jambert, C., Cellier, P. & Delmas, R. 1999. Nitrous oxide fluxes from a fertilised maize crop using micrometeorological and chamber methods. *Agricultural & Forest Meteorology*, **96,** 19-38.

Laville, P., Lehuger, S., Loubet, B., Chaumartin, F. & Cellier, P. 2011. Effect of management, climate and soil conditions on N_2O and NO emissions from an arable crop rotation using high temporal resolution measurements. *Agricultural & Forest Meteorology*, **151,** 228-240.

Levy, P.E., Gray, A., Leeson, S.R., Gaiawyn, J., Kelly, M.P.C., Cooper, M.D.A., *et al.* 2011. Quantification of uncertainty in trace gas fluxes measured by the static chamber method. *European Journal of Soil Science*, **62,** 811-821.

Livingston G. & Hutchinson G. 1995. Enclosure-based measurement of trace gas exchange: applications and sources of error. *Biogenic trace gases: measuring emissions from soil and water***,** 14-51. Blackwell Science, Cambridge University Press, Cambridge.

420 Parkin, T.B., Venterea, R.T. & Hargreaves, S.K. 2012. Calculating the detection limits of
421 chamber-based soil greenhouse gas flux measurements. *Journal of Environmental Quality*,
422 **41,** 705-715.
423 Pedersen, A.R., Petersen, S.O., & Schelde, K. 2010. A comprehensive approach to soil-
424 atmosphere trace-gas flux estimation with static chambers. *European Journal of Soil*
425 *Science*, **61,** 888-902.
426 Ravishankara, A.R., Daniel, J.S. & Portmann, R.W. 2009. Nitrous oxide (N_2O): the dominant
427 ozone-depleting substance emitted in the 21st century. *Science*, **326,** 123-125.
428 Velthof, G.L., Jarvis, S.C., Stein, A., Allen, A.G. & Oenema O. 1996. Spatial variability of
429 nitrous oxide fluxes in mown and grazed grasslands on a poorly drained clay soil. *Soil*
430 *Biology & Biochemistry*, **28,** 1215-1225.
431 Yamulki, S. & Jarvis, S.C. 1999. Automated chamber technique for gaseous flux
432 measurements: Evaluation of a photoacoustic infrared spectrometer-trace gas analyzer.
433 *Journal of Geophysical Research-Atmospheres*, **104,** 5463-5469.
434 Zahniser, M.S., Nelson D.D., McManus J.B., Herndon S.C., Wood E.C., Shorter J.H., *et al*.
435 2009. Infrared QC laser applications to field measurements of atmospheric trace gas
436 sources and sinks in environmental research: enhanced capabilities using continuous wave
437 QCLs. *Quantum Sensing & Nanophotonic Devices VI*, **7222**.
438

Figure Captions

Figure 1 Schematic diagram of the dynamic chamber used for more detail.

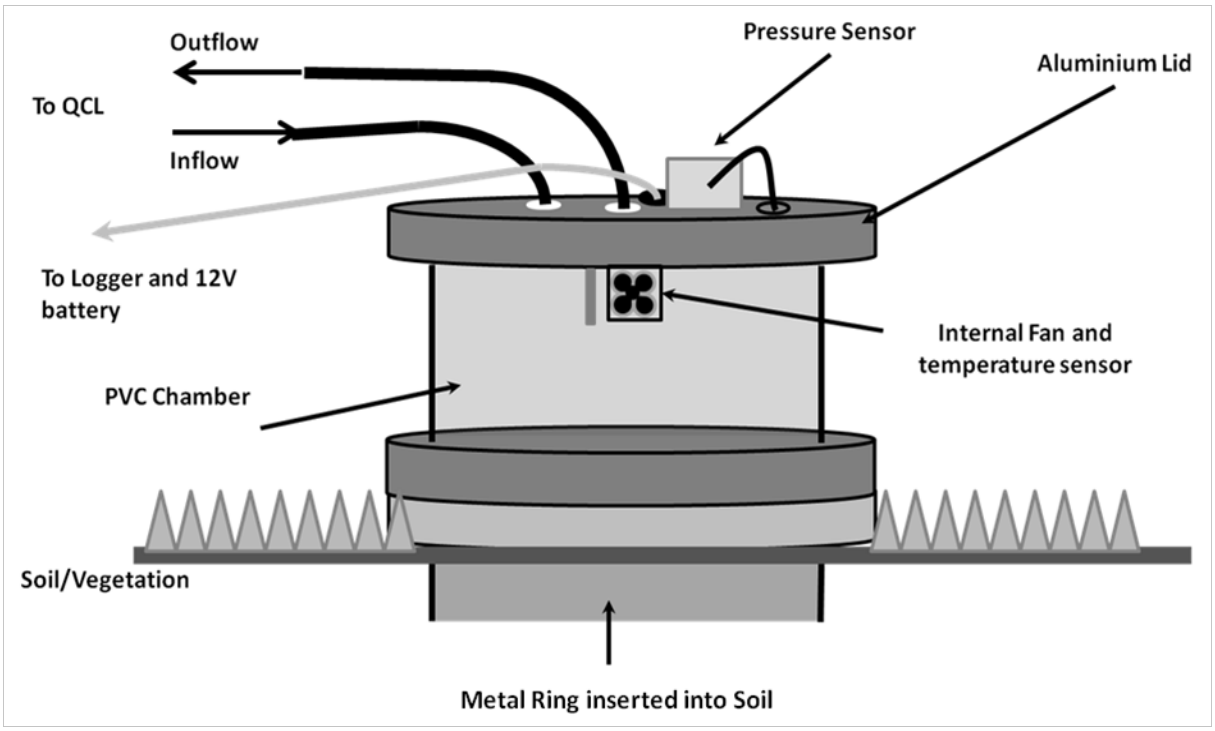

Figure 2 Example of N_2O concentration measurements affected by wind over a 30-minute period without the use of the wind-blocking skirt. Concentration changes within the chamber should look close to linear (as in Figure 3), but an influence of gusts is apparent. The effect is more obvious when greater gas concentrations are present within the chamber. Measurement made on mown grass with added ammonium nitrate, at CEH Edinburgh, UK, March 2012.

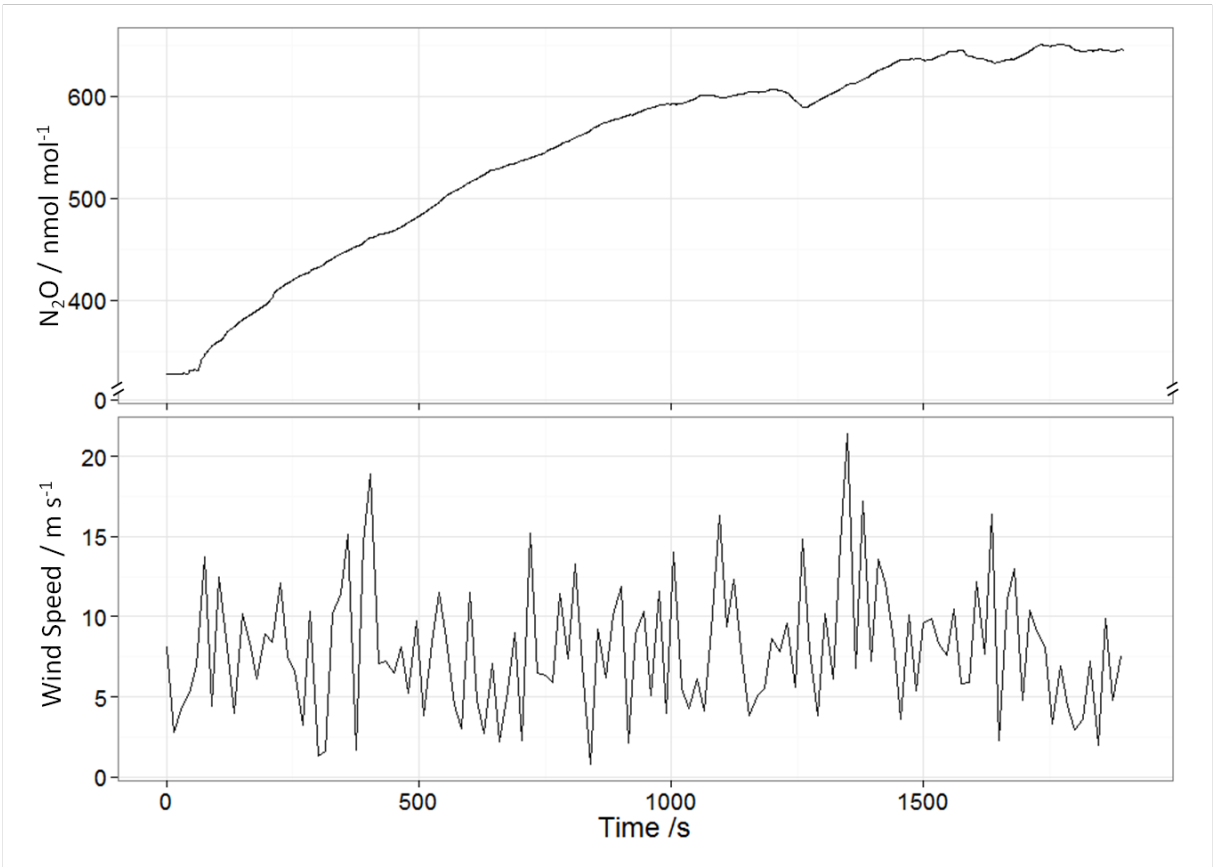

Figure 3 Example of N_2O and CO_2 concentration measurements recorded at 1 Hz by a QCL during three chamber measurements using the dynamic chamber from three different nearby locations within close range. Fluxes are calculated from the change in concentration over time. Each measurement lasts approximately 180 seconds of which the first 60 seconds are discarded from the regression analysis. Measurements were made on multiple grassland plots with synthetic urine fertiliser applied. (Crichton, Dumfries, SW Scotland, November 2012)

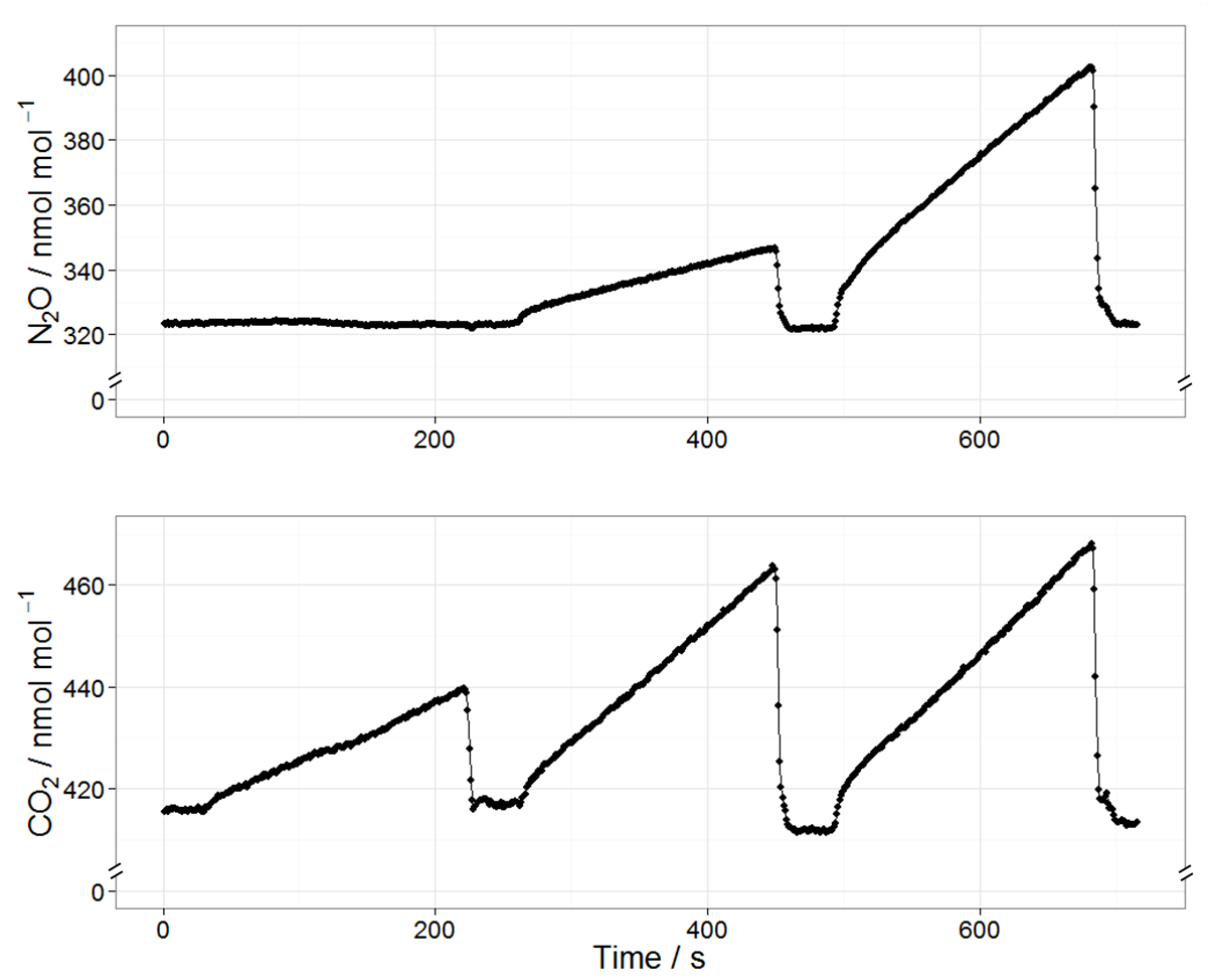

Figure 4 *C*oncentration increase over time within the chamber over the course of 20 hour-long measurements. The plots are ranked in order of magnitude of flux, increasing top-left (#13) to bottom-right (#20), labelled by an arbitrary measurement number. Measurement

made on mown grass with added ammonium nitrate on 16 of the 20 plots (see Table 1): CEH Edinburgh, March 2012.

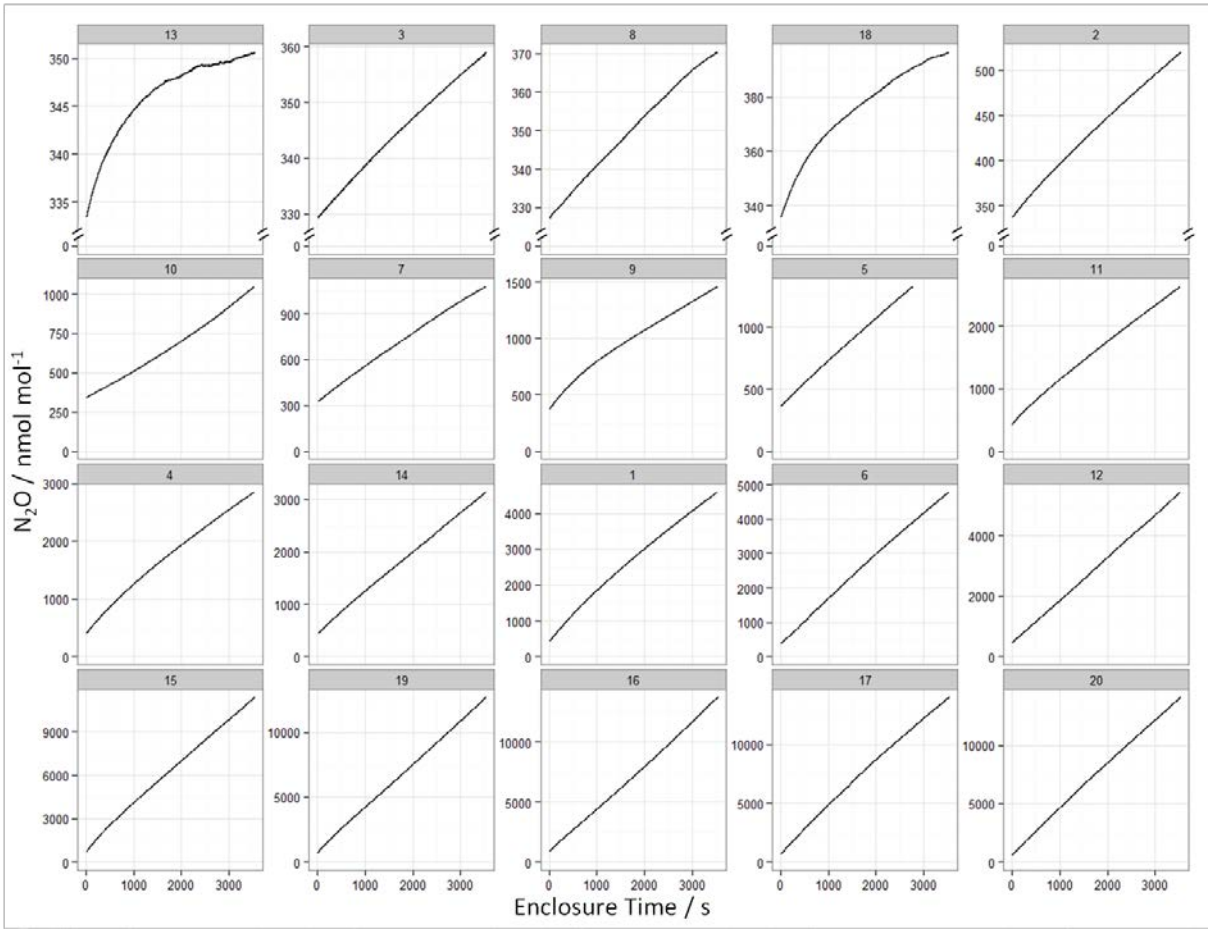

Figure 5 Fluxes calculated from the hour-long measurements (from Figure 4) over a range of possible enclosure times, and with both linear and nonlinear fitted models. Note that the fluxes are all shown on the same absolute scale.

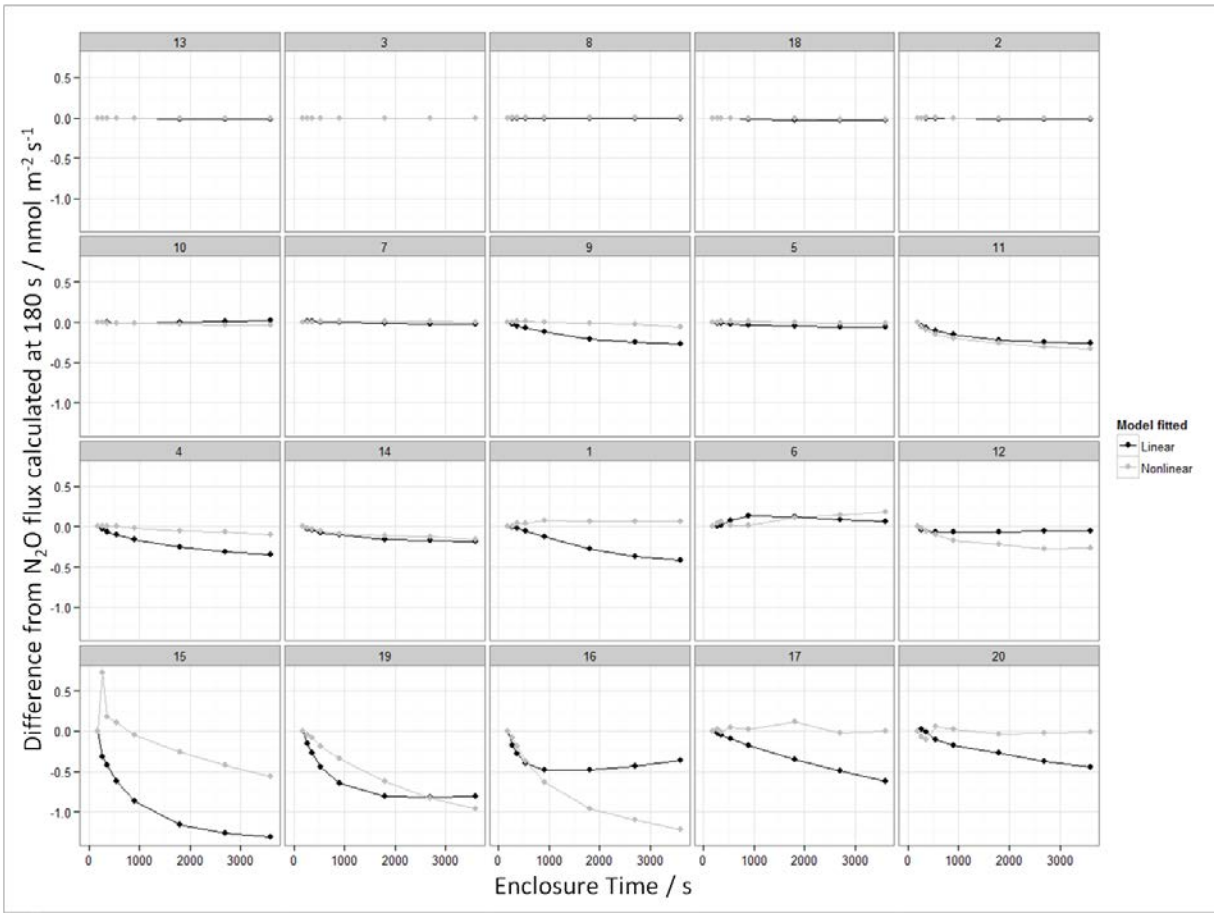

Figure 6 A direct comparison of N_2O flux measurements made using the dynamic and static chamber methods at a SRUC field site in Dumfries (October to November 2012). The dashed line represents the 1:1 relationship. The dotted line is the line of least-squares best fit through all data points.

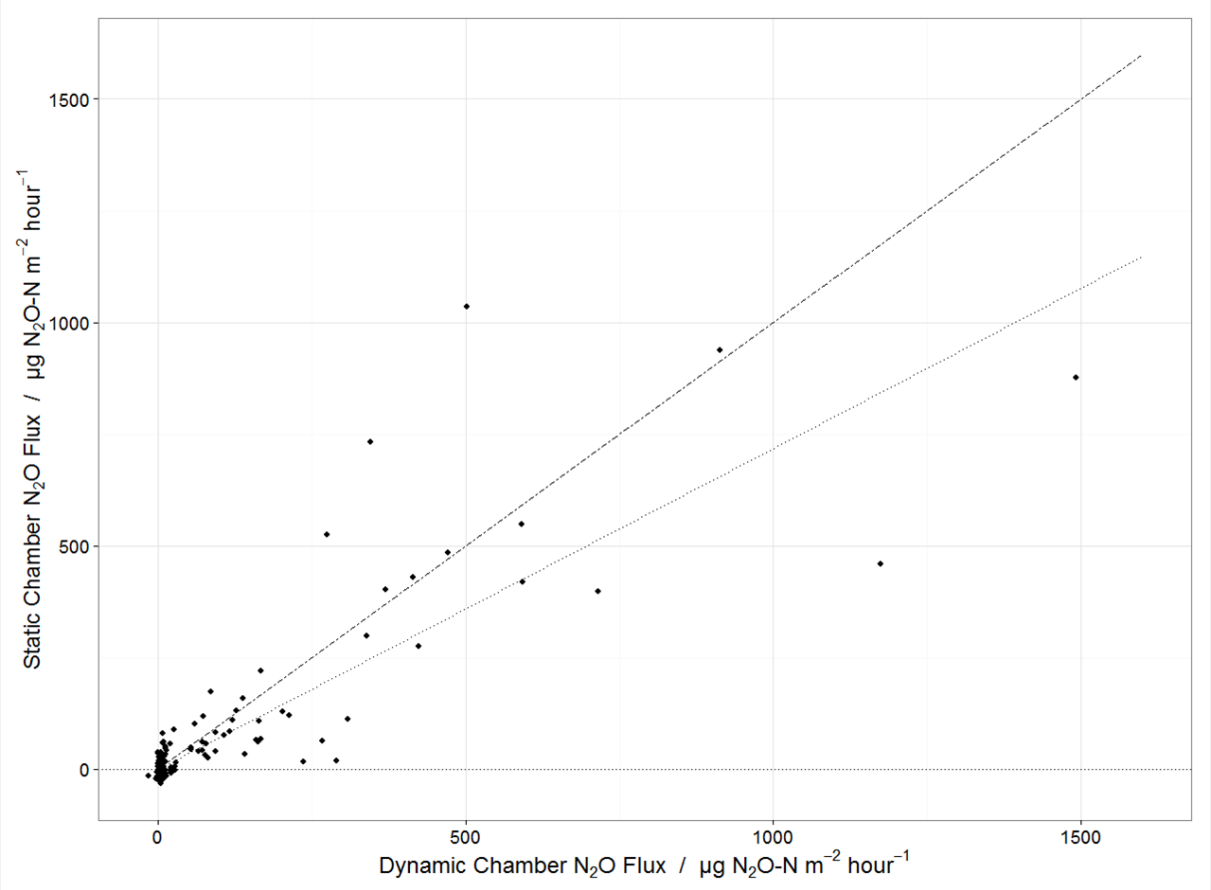

Figure 7 A comparison of N_2O fluxes measured from untreated control plots using both dynamic and static chamber methods. The box plot represents the 25th and 75th percentile ranges. The ability of the dynamic chamber method to measure background flux precisely is highlighted by the small range of uncertainty.

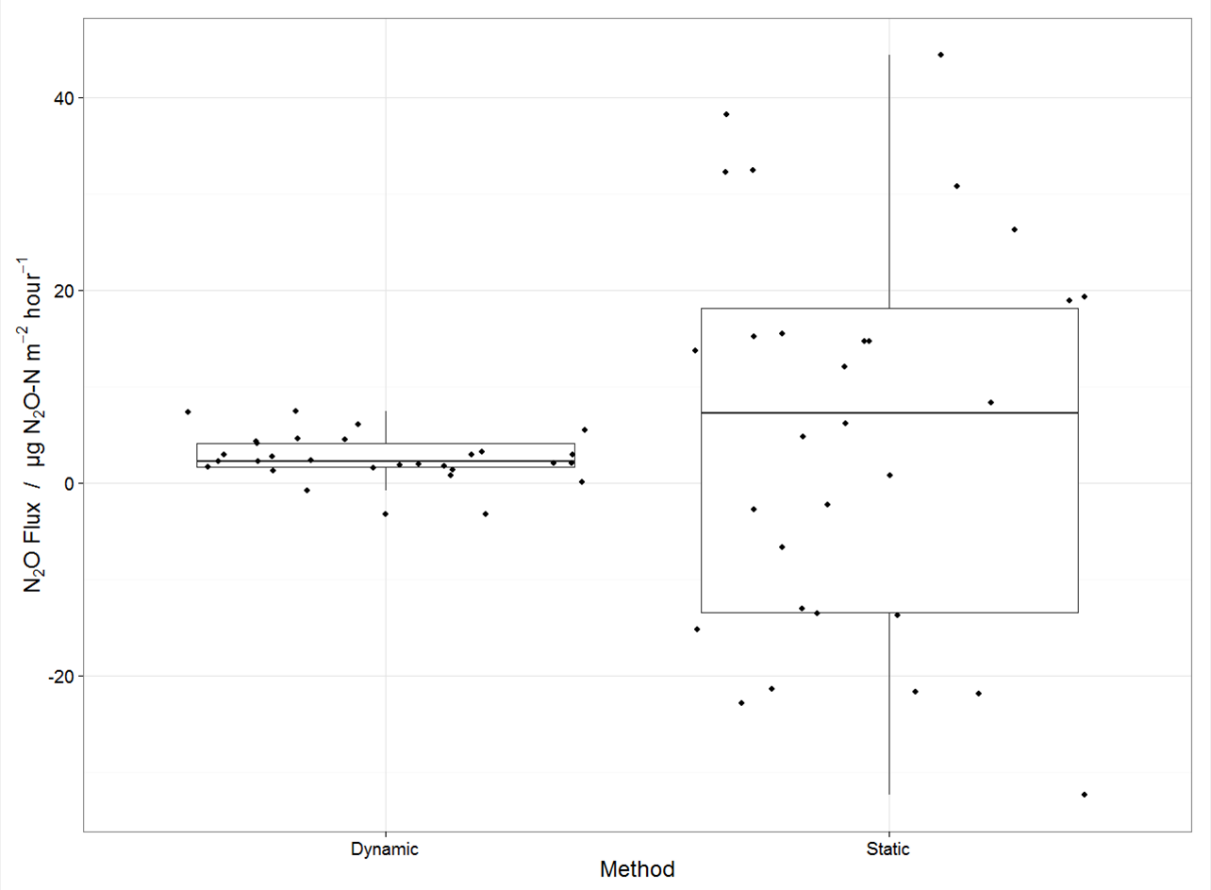

Figure 8 A representation of all of the calculated uncertainties made using the dynamic chamber method at the Crichton field site. The estimated uncertainty in dC/dt in static chambers (20%) is added as a comparison with literature estimates (Levy *et al.*, 2011). The results demonstrate the improved ability to measure dC/dt precisely using the dynamic chamber method.

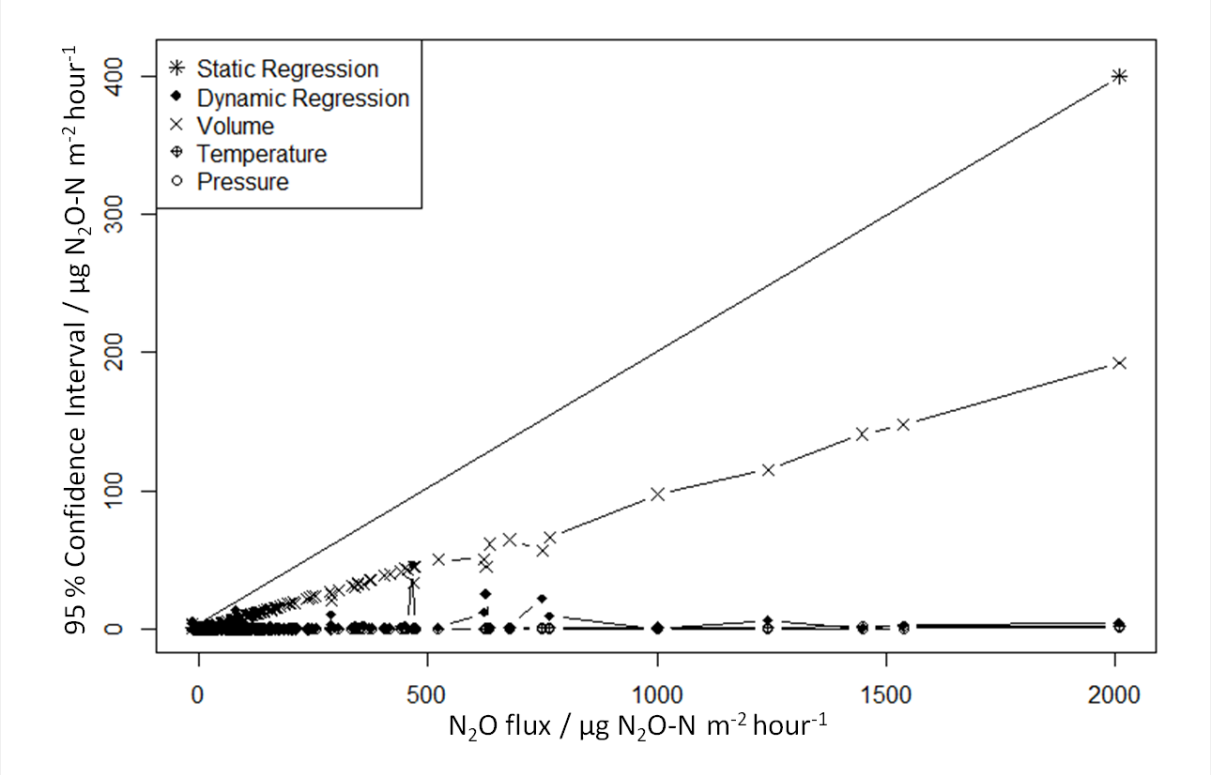

494 **Table 1** A comparison of N_2O fluxes (µg N_2O-N m^{-2} $hour^{-1}$) calculated using linear and non-
495 linear regression from hour long measurements using the dynamic chamber method. The table
496 is arranged in order of increasing flux.

		Linear			Non-linear		
Plot number	Added N Treatment	Flux	95% confidence interval	R^2	Flux	95% confidence interval	R^2
13	N	3.9	124.5	0.84	17.4	1.3	0.98
3	N	8.7	13.5	0.99	10.2	0.2	0.99
8	N	12.9	14.1	0.99	14.9	0.6	0.99
18	N	15.7	69.5	0.95	35.4	2.0	0.99
2	Y	52.9	13.9	0.99	62.3	0.3	0.99
10	Y	204.3	20.1	0.99	230.2	3.0	0.99
7	Y	219.7	9.6	0.99	248.3	0.3	0.99
9	Y	298.1	31.8	0.99	424.7	1.3	0.99
5	Y	362.5	0.5	0.99	405.2	0.0	0.99
11	Y	627.5	12.3	0.99	718.9	0.4	0.99
4	Y	705.1	21.4	0.99	905.7	0.5	0.99
14	Y	780.6	6.0	0.99	881.8	0.7	0.99
1	Y	1202.9	19.5	0.99	1508.9	0.5	0.99
6	Y	1277.4	8.8	0.99	1443.7	0.3	0.99
12	Y	1440.3	2.0	0.99	1626.4	1.1	0.99
15	Y	3048.6	9.6	0.99	3445.4	0.6	0.99
19	Y	3419.8	3.2	0.99	3861.6	1.1	0.99
16	Y	3707.8	6.6	0.99	4184.4	1.6	0.99
17	Y	3849.8	11.9	0.99	4427.8	0.2	0.99
20	Y	3922.9	6.7	0.99	4432.7	0.4	0.99

497

498 Table 2 Cost-benefit analysis of QCL dynamic chamber and GC static chamber methods.

	QCL Dynamic Chamber	GC Static Chamber
Capital cost	€ 120 k	€ 18 k
Flux measurement time (minutes)	5	60
Number of simultaneous measurements	1	up to 10
Laboratory analysis time (minutes)	0	60
Number of measurements per hour of effort	12	5
Uncertainty (95 % CI) (μg N_2O-N m^{-2} $hour^{-1}$)	2	20

499